Supporting Information

Developing Three-Dimensional Co-Continuous Phase Network Structure via the enhanced Inter-component Affinity for High-Performance Flexible Organic Radical Electrodes

*Yaoguang Chen, Xiu Liu, Zhengqi Lao, Kang Yang, Fuzhen Li, Ling Chen, Kancheng Mai and Zishou Zhang**

Key Laboratory for Polymeric Composite and Functional Materials of Ministry of Education
Key Laboratory of High Performance Polymer-based Composites of Guangdong Province, School of Chemistry
Sun Yat-sen University
Guangzhou, 510275, China
*Corresponding authors: zhzish@mail.sysu.edu.cn

Synthesis and characterization of PETM and PTMA.

Poly (ethylene-alt-TEMPO maleate) (PETM) was synthesized through moderate esterification between Poly (ethylene-alt-maleic anhydride) (PEM) and 4-hydroxy-TEMPO under the catalysis of 4-dimethylaminopyridine (DMAP)/ 2-chloro-1-methyl-pyridinium iodide (CMPI)/ triethylamine (TEA) in mixed solvents of dichloromethane and acetone according to our previous report, as is illustrated in Fig. S1. [1]

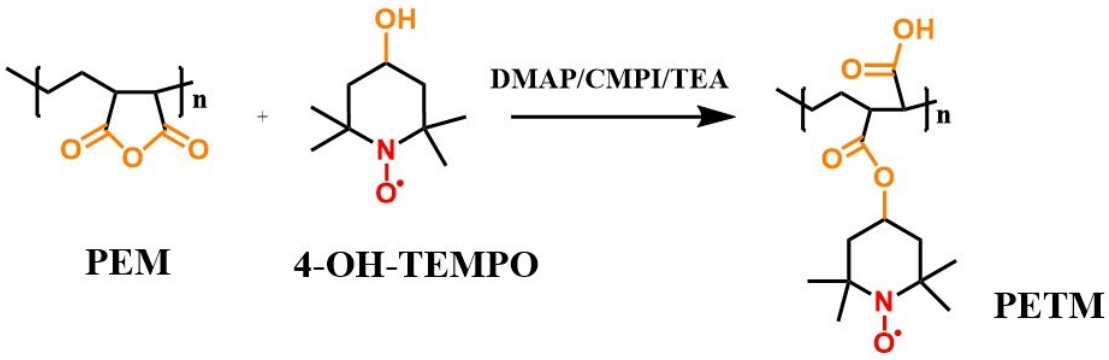

Fig. S1 Schematic illustration of the synthesis of PETM.[1]

To investigate the chemical structure of PETM, FI-IR was conducted and the spectrum was shown in Fig. S2. The characteristic peaks at 1726 cm^{-1}, 1176 cm^{-1}, and 1365 cm^{-1} were attributed to C=O, C-O-C, and N-O• respectively.[2, 3] Besides, the peaks at 2976 cm^{-1} and 2941cm^{-1} represent -CH_2- and -CH_3 respectively, while the wide peak at 3550-3200 cm^{-1} corresponded to the -OH of the carboxyl groups. These findings suggested the existence of TEMPO, carboxyl groups, and ester groups in PETM as depicted in Fig. S1.[1]

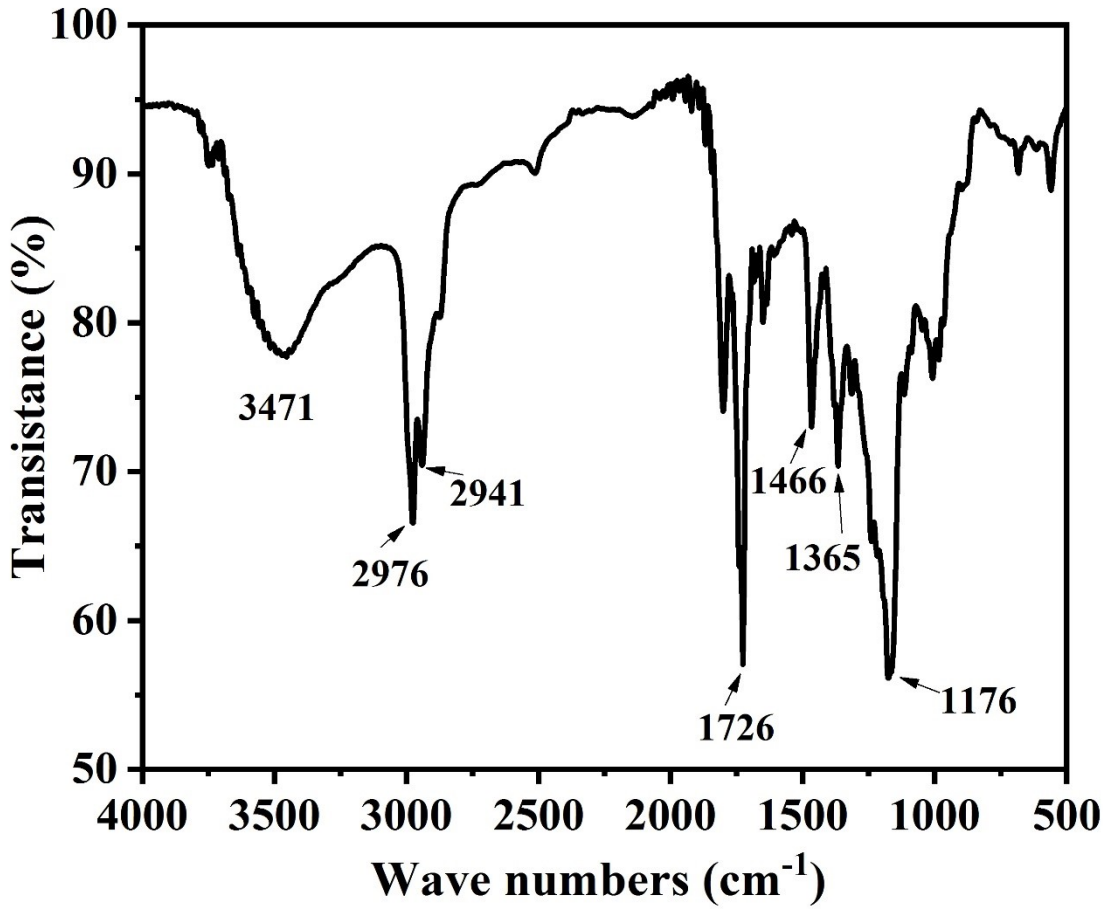

Fig. S2 The FT-IR spectra of PETM.

To calculate the radical concentration of PETM, Element Analysis (EA) and Physical Property Measurement System (PPMS) were conducted based on the typical N content and magnetic susceptibility of TEMPO, respectively. When $N > 4.70\%$, PETM mainly consists of the repeat unit a and b in Fig. S3. According to the equation S1, S2, and S3, C_{rad} was calculated as 1.10 unpaired electrons per unit in PETM, as shown in Table S1.[1]

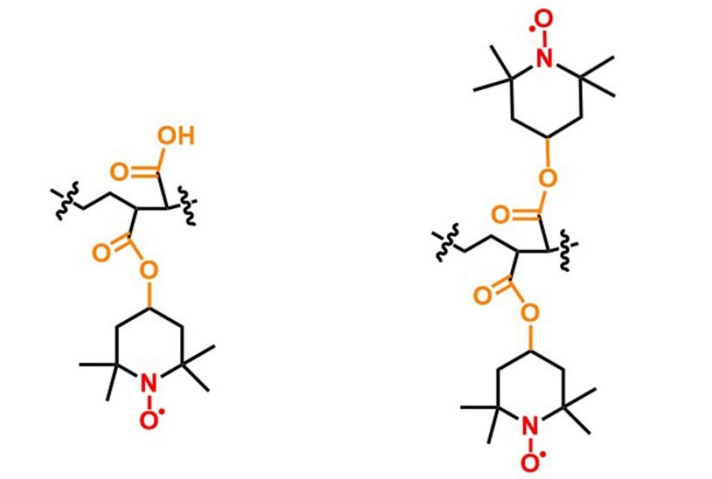

Fig. S3 The main repeat units in PETM.

$$4.7\% \times 298 \times n_b + 6.19\% \times 452 \times n_a = N \times m \quad \text{S1}$$

$$298 \times n_b + 452 \times n_a = m \quad \text{S2}$$

$$C_{rad} = \frac{2 \times n_a + n_b}{n_b + n_c} \quad \text{S3}$$

where n_b, n_a, N, m, and C_{rad} represent the moles of the unit a and b, the nitrogen content, mass, and radical concentration of PETM, repsectively.

Table S1. The EA results of PETM.

	C (%)	H (%)	N (%)	C_{rad} (numders / per unit)
PETM	62.17	8.48	4.92	1.10

The PPMS results was shown in Fig. S4. The good linear dependence of the fitting curve indicated the completely paramagnetic behavior of PETM. According to the slope of the fitting curve, 1.08 unpaired electrons per repeating unit of PETM was obtained,[1, 4] which was close to the EA result, and then the theoretical capacity was calculated as 94 mAh g^{-1} based on the equation S4.

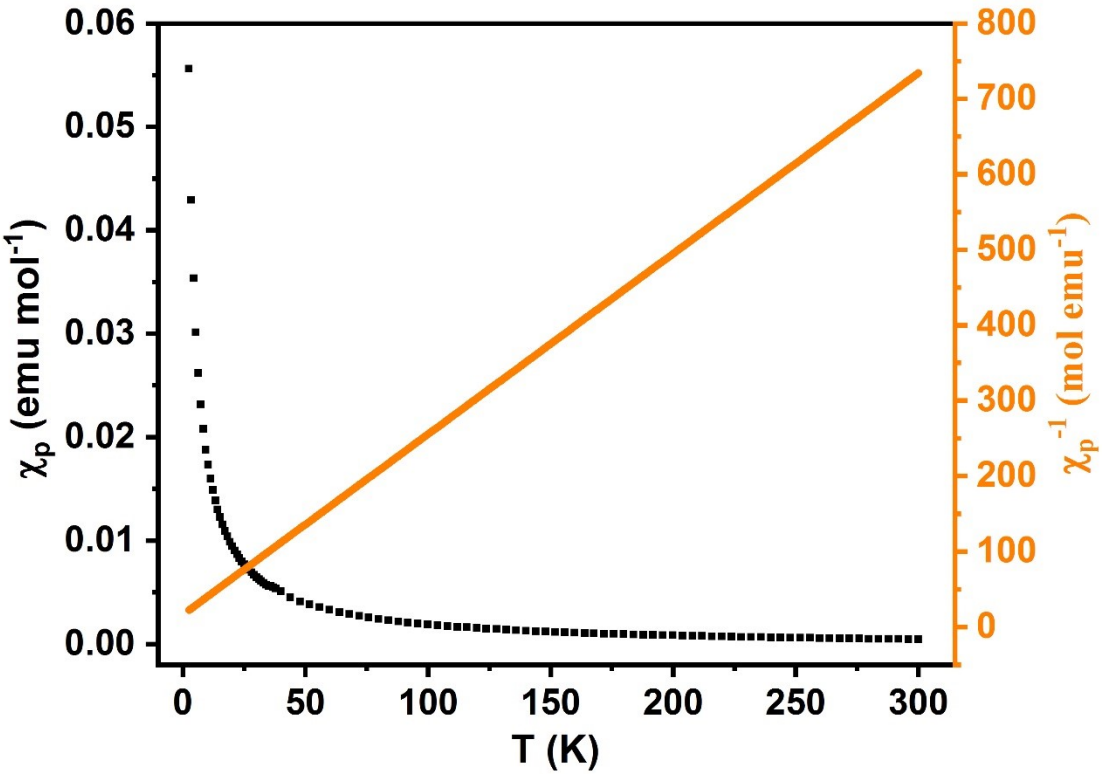

Fig. S4 Curie-Weiss plots of PETM (dark gray) and the fitting curve (orange) of the reciprocal of χ_p (low-temperature paramagnetic susceptibility) as a function of temperature.

The theoretical capacity of radical polymers was based on the equation S4.

$$C\ (mA\ h/g) = \frac{1000\ \times\ n\ \times\ F}{3600\ \times\ M_w} \qquad \text{S4}$$

where F represents the Faraday constant (96484 C/mol), n is the exchanging electron numbers per repeating unit, and M_{w} is the molecular weight of the repeating unit of radical polymers.

PTMA was synthesized through the radical polymerization of 2,2,6,6-tetramethylpiperidine methacrylate (MTMP) monomer and the subsequent oxidation process, as shown in Fig. S5.[3]

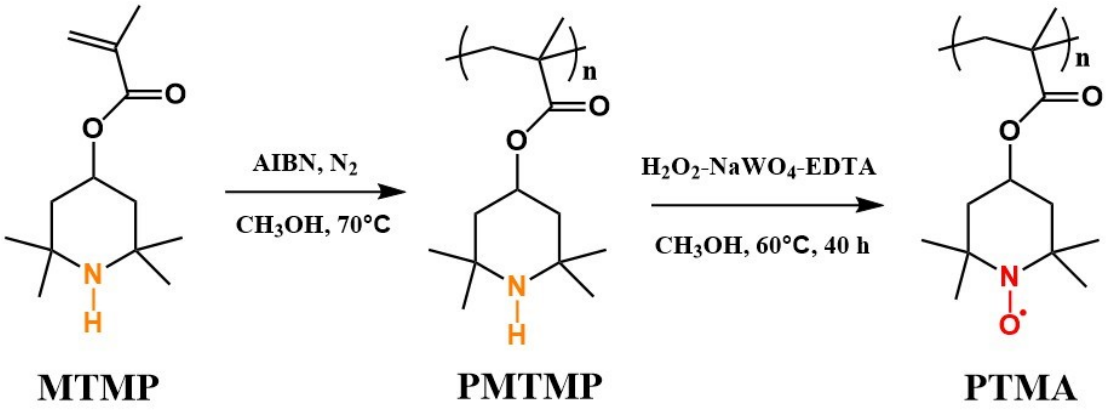

Fig. S5 Schematic illustration of the synthesis of PTMA.

Due to the easy dissolution of PTMA in many common solvents, Ultraviolet–visible (UV) spectroscopy is a simple and efficient way to determine its radical concentration[5] with the results demonstrated in Fig. S6. Taking the peak height of the UV spectrum of PTMA into the fitted equation in Fig. S6c, the radical concentration was calculated as 1.00 unpaired electrons per repeating unit.

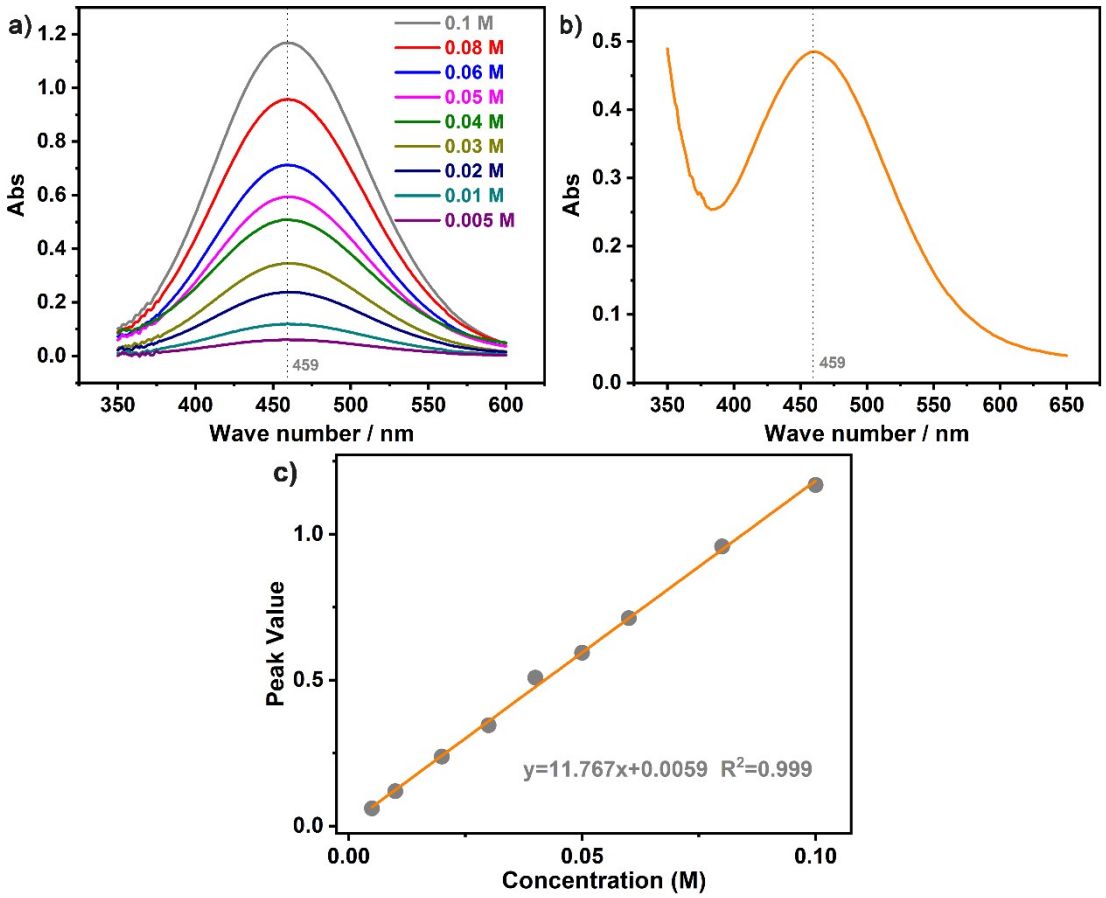

Fig. S6 a) UV spectrum of standard TEMPO solution in dichloromethane with a series of concentrations including 0.1, 0.08, 0.06, 0.05, 0.04, 0.03, 0.02, 0.01, and 0.005 M; b) UV spectra of 0.482 mg PTMA in 50 mL dichloromethane; c) Calibration curve based on the peak height at 459 nm of standard TEMPO solution, demonstrating a good linear dependence (R^2=0.999).

Besides, PPMS was performed to calculate the radical concentration of PTMA with the result displayed in Fig. S7. The linear fitting curve suggested the paramagnetic behavior of PTMA, and the radical concentration was calculated as 0.85 unpaired electrons per repeating unit. The different values given by UV and PPMS may be due to the errors of different method, which has been reported before as well.[5] Assuming the radical concentration of PTMA was 0.85-1.00, its theoretical capacity was determined as 96-112 mA h/g.

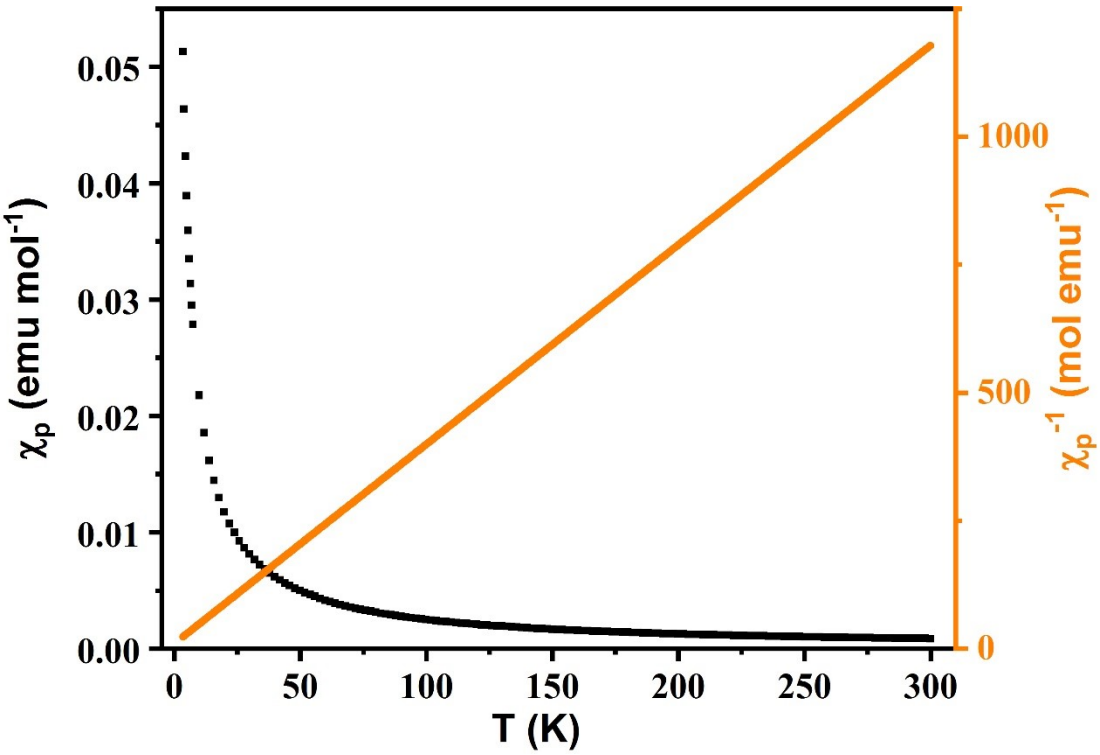

Fig. S7 Curie-Weiss plots of PTMA (dark gray) and the fitting curve (orange) of the reciprocal of χ_p (low-temperature paramagnetic susceptibility) as a function of temperature.

Molecular dynamic simulation and calculation details

In the first system, the canonical ensemble (NVT) was used and the temperature was monitored by the Nose-Hoover algorithm. In order to make the radical polymers melt and accelerate the absorption process of the radical polymers on carbon nanotubes, the temperature was maintained at 500 K at first, running 2 million steps, and then gradually cooled down to 300 K after running 1 million steps. Finally, the temperature was kept at 300 K and ran 0.5 million steps. For the second system, the isothermal-isobaric ensemble was used. Both the air pressure and the temperature were controlled by the Nose-Hoover algorithm, while the air pressure was maintained at 1 Atmosphere. The running program was the same as the first system. The step time of all simulations was 1 fs and the truncation distance of the potential accorded to 1 nm. Additionally, atom numbers of PETM (or PTMA) within a distance of 3.34 Å on the surface of SWNT were counted and the simulation results were visualized by Ovito 3.0.[6] The microstructures of a) PETM/SWNT and b) PTMA/SWNT in the second system were shown in Figure S 9a and S 9b, respectively.

The van der Waals interactions between radical polymers and carbon nanotubes are defined as:

$E_{inter} = E_{total} - (E_{poly} + E_{SWNT})$

Where E_{total} is the total energy of the system (PETM/SWNT or PTMA/SWNT), E_{poly} is the energy of the radical polymers, E_{SWNT} is the energy of the carbon nanotubes, respectively. On the basis of the definition, the negative values of E_{inter} suggest an exothermic process. In addition, the higher negative values mean stronger interaction between the radical polymers and the carbon nanotubes.

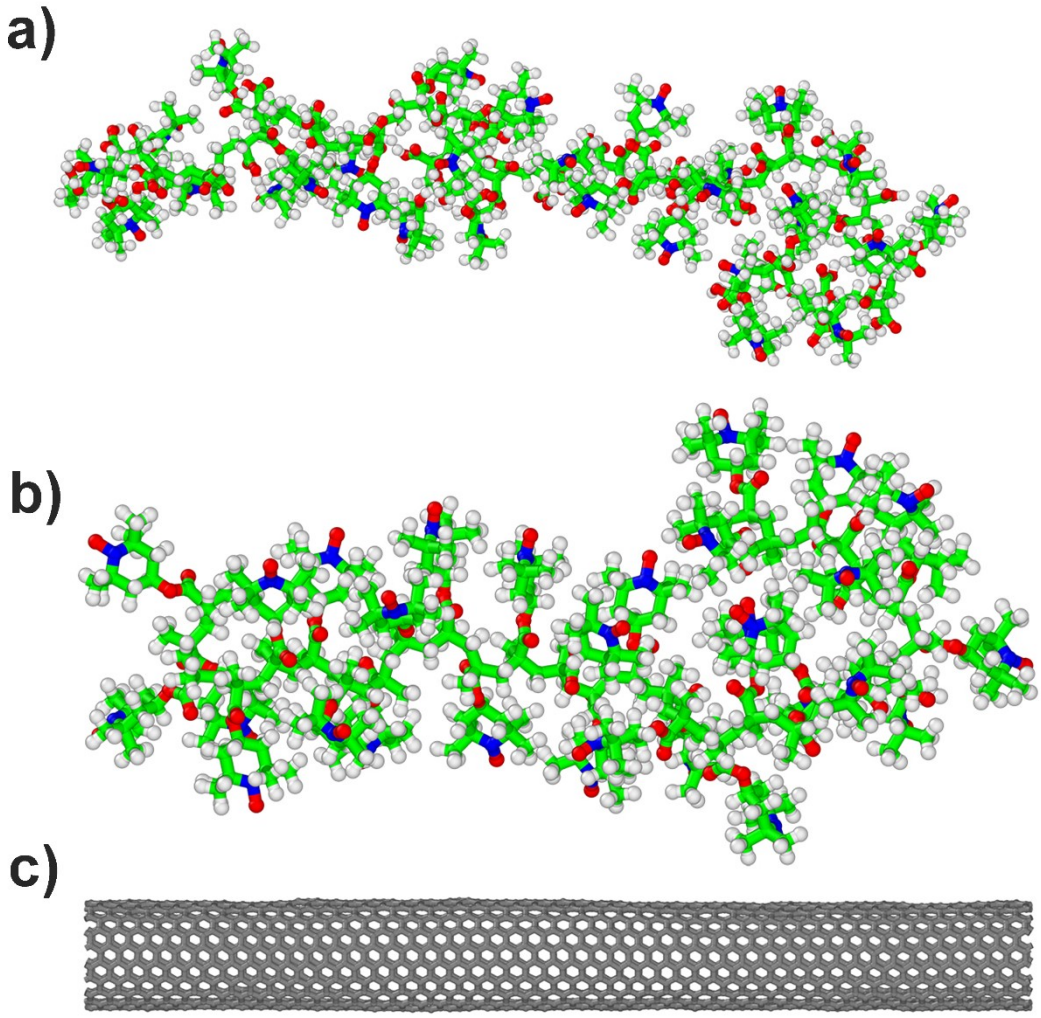

Fig. S8 The molecular models of a) PETM, b) PTMA, and c) SWNT (the red, green, blue, and gray represent the O, C, N, and H atoms respectively).

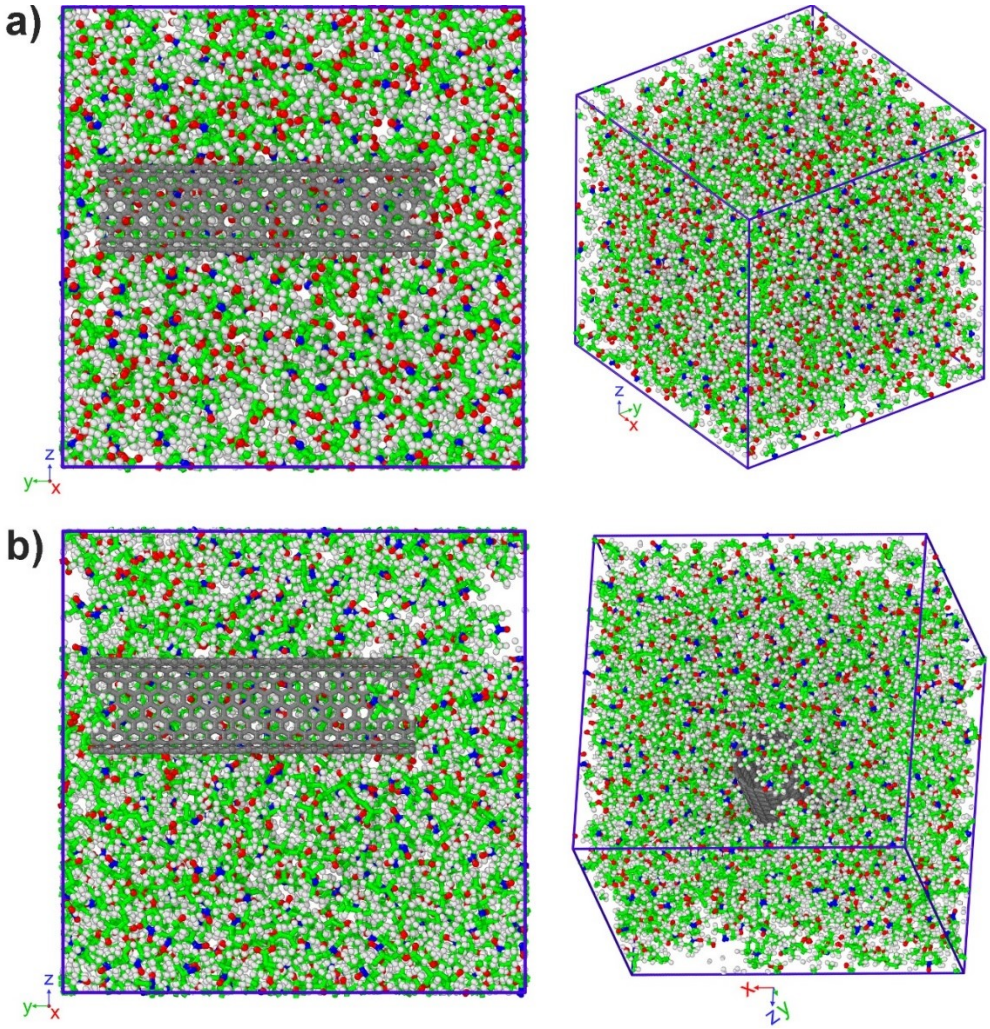

Fig. S9 The microstructures of a) PETM/SWNT and b) PTMA/SWNT in the second system for energy calculation.

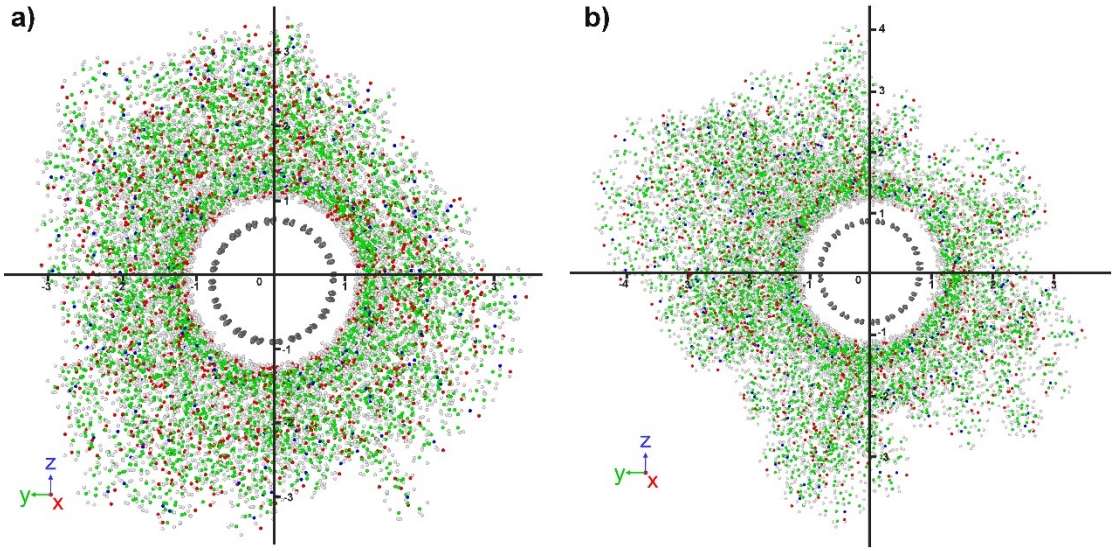

Fig. S10 Projective images of the atomic spatial distribution for a) PETM/SWNT and b) PTMA/SWNT with distance in nm. (The red, green, blue, and gray represent the O, C, N, and H atoms respectively).

Table S2 The atom numbers of PETM (or PTMA) within a distance of 3.34 Å on the surface of SWNT.

Numbers / Systems	**H atoms**	C atoms	O atoms	**The red H atoms from the TEMPO group**	**The blue H atoms from the TEMPO group**	The orange H atoms in the backbone	The green H atoms in the methyl side chain
PETM/CNT	**513.5**	9.5	110.1	**353.8**	**158.8**	0.5	0.0
PTMA/CNT	**464.0**	13.8	41.1	**280.8**	**86.3**	13.2	83.8

Table S3 The van der Waals interactions between the radical polymers and the carbon nanotubes

System	E_{total} [kcal/mol]	E_{poly} [kcal/mol]	E_{SWNT} [kcal/mol]	E_{inter} [kcal/m^2]
PETM/CNT	-14264.60	-12231.00	-967.43	-3.43
PTMA/CNT	-11416.20	-9561.98	-966.36	-2.84

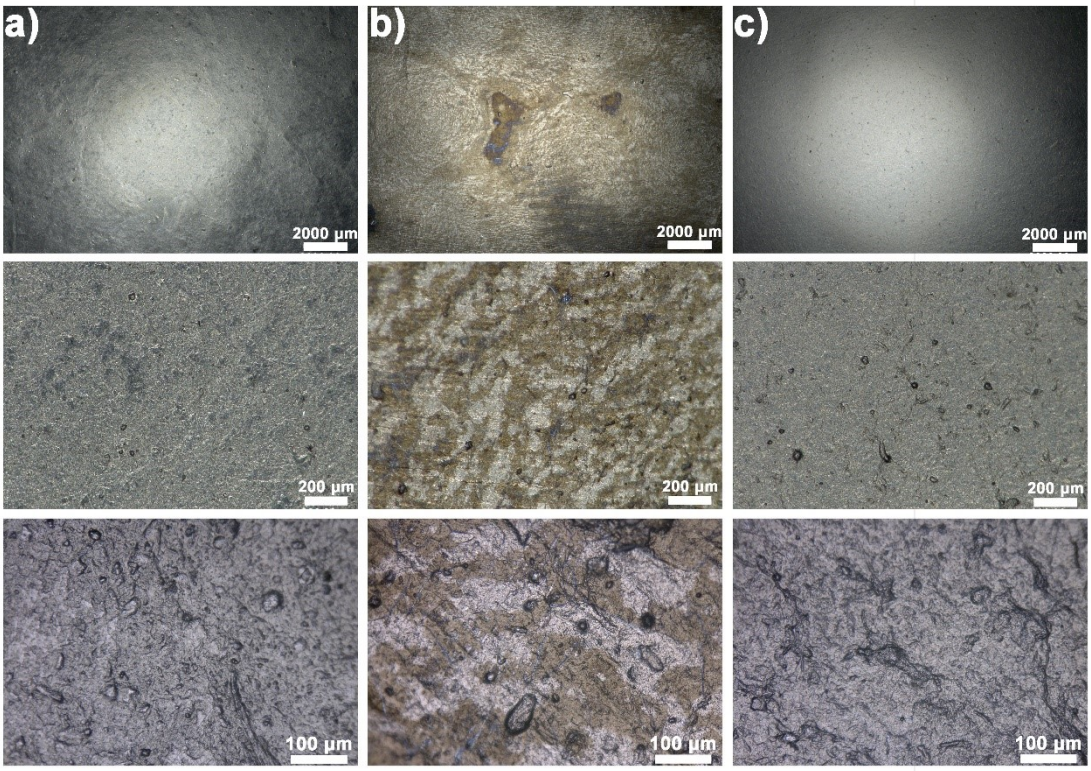

Fig. S11 Ultra-depth microscope images of a) pure SWNT film, b) PTMA/SWNT film, and c) PETM/SWNT film, showing the evident agglomeration in PTMA/SWNT while the others have a uniform gray color in appearance.

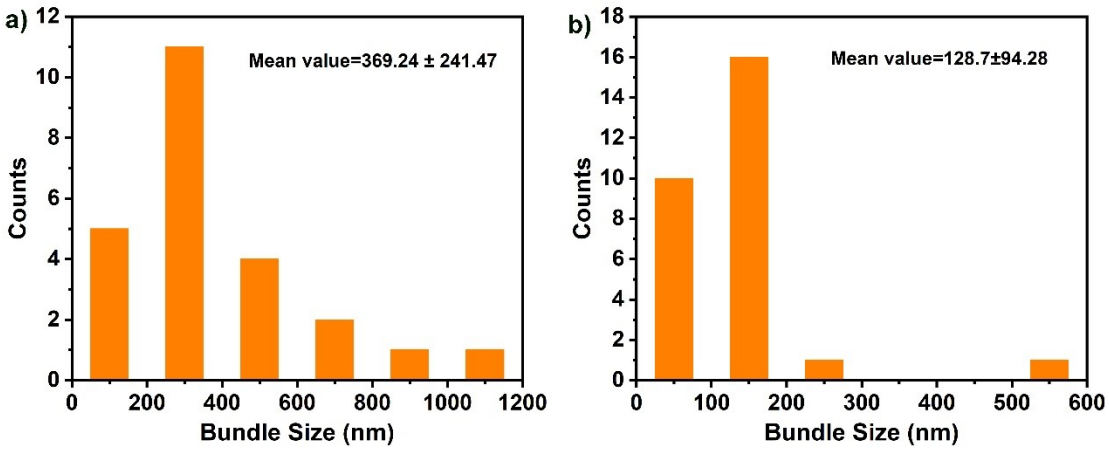

Fig. S12 The size distribution of SWNT bundle for a) pure SWNT and b) PETM/SWNT films obtained from the corresponding SEM images in Fig. 3e and g.

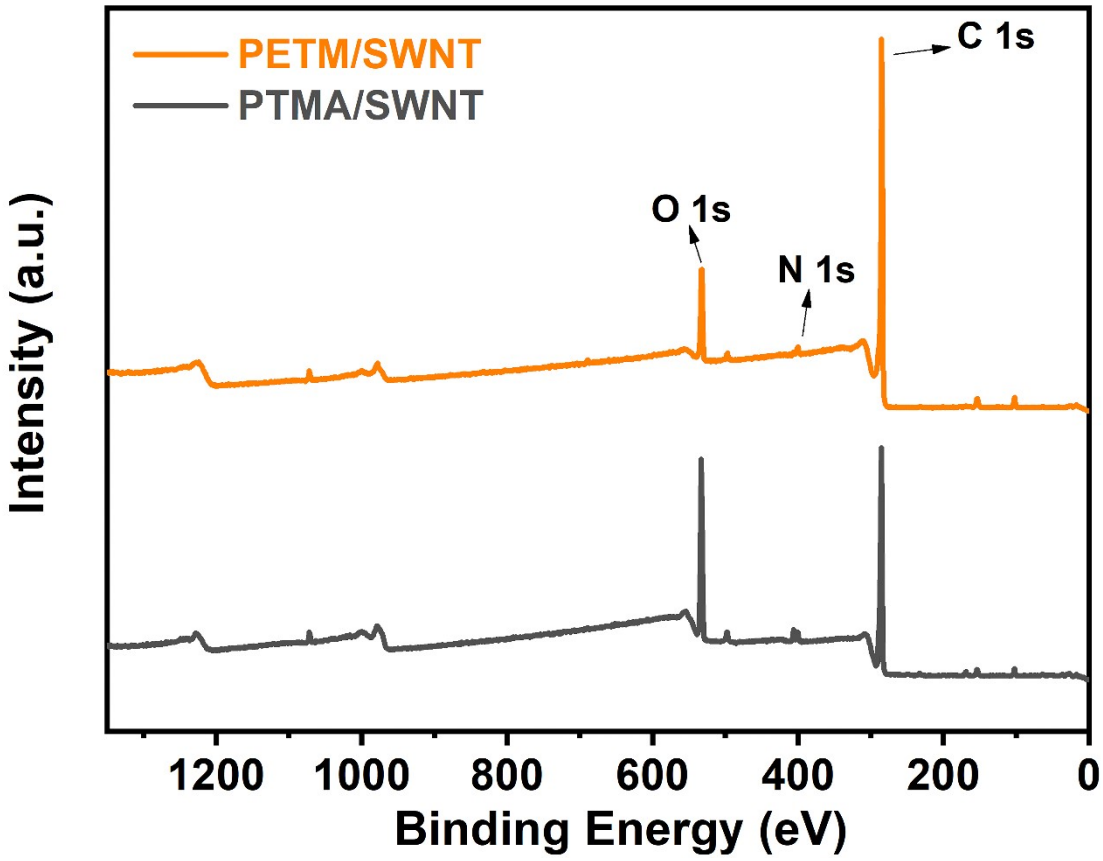

Fig. S13 XPS survey spectra of the PETM/SWNT and PTMA/SWNT.

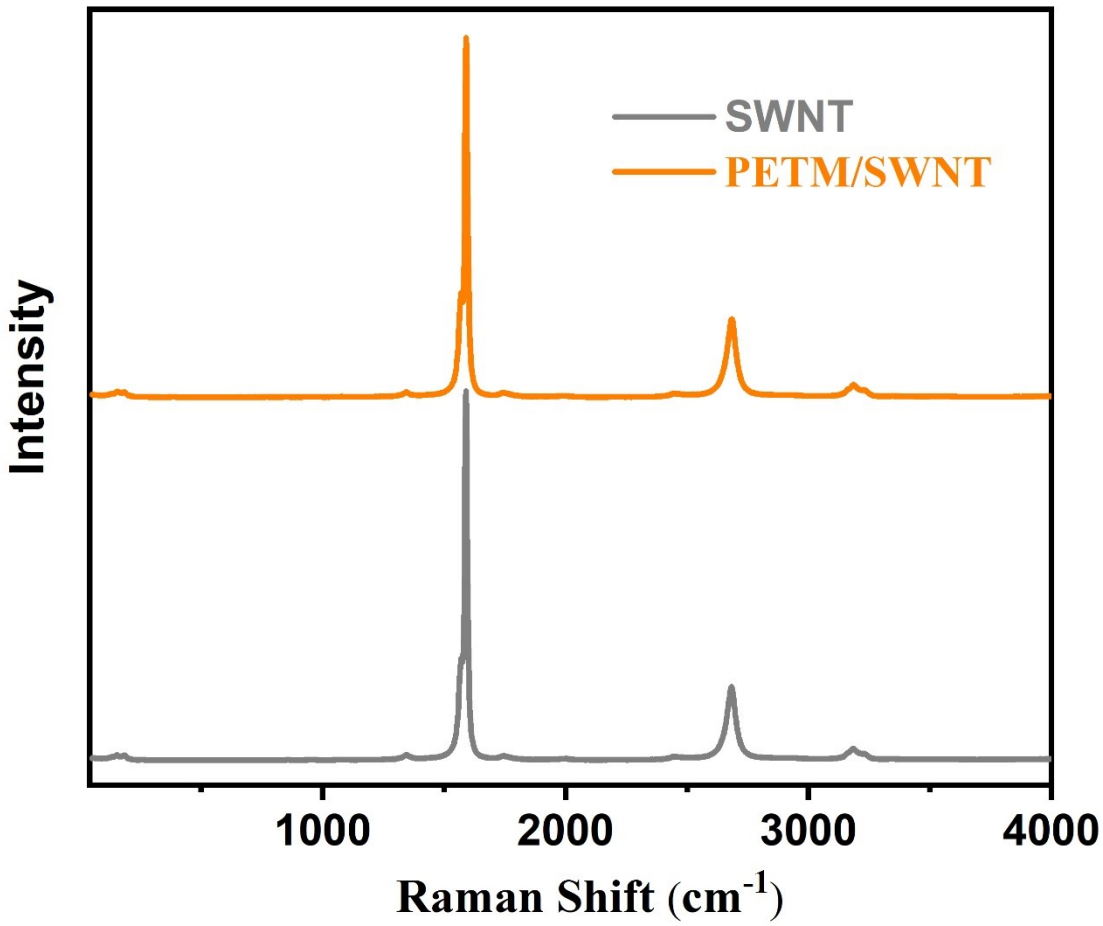

Fig. S14 Raman spectra of pure SWNT and PETM/SWNT films.

Table S4 Mechanical index of pure SWNT film and PETM/SWNT film.

	Elongation at break [%]	Tensile strength [MPa]
Pure SWNT	2.88±0.33	28.11±2.84
PETM/SWNT	1.24±0.28	50.30±4.79

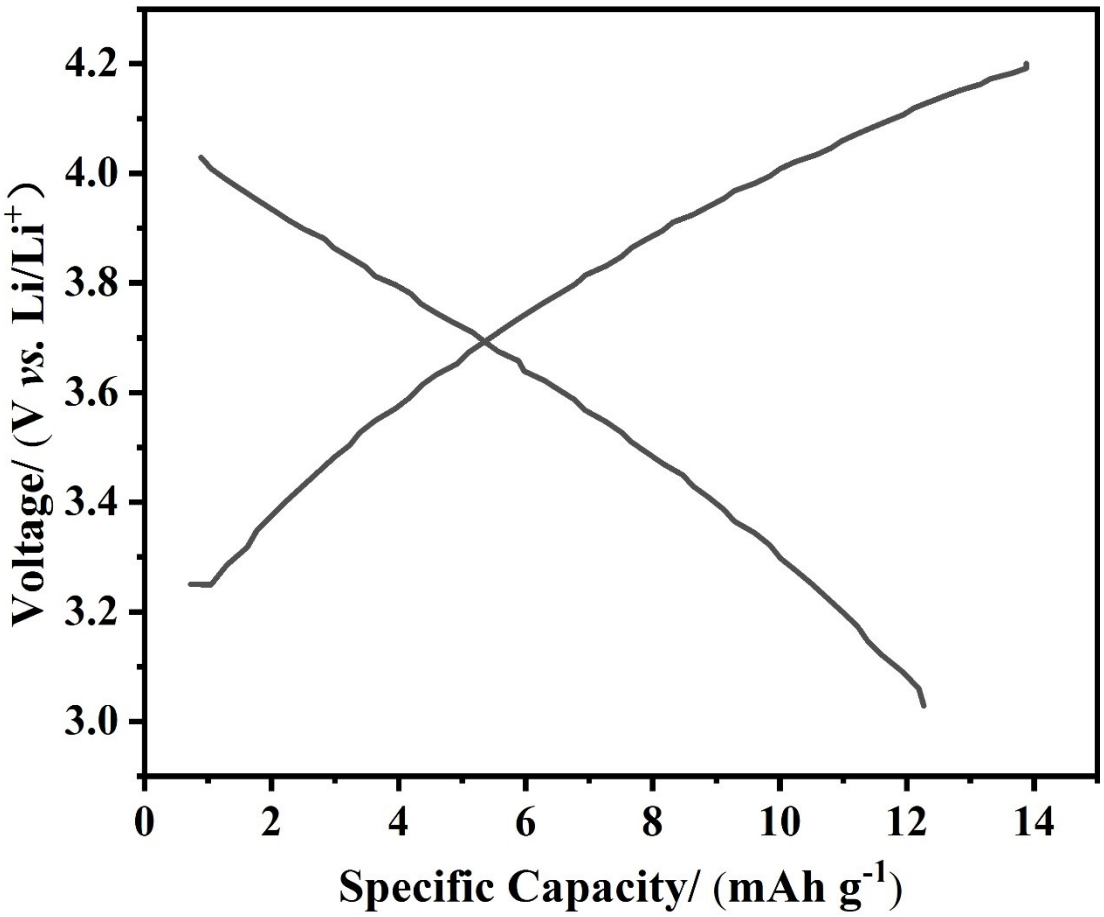

Fig. S15 Galvanostatic charge-discharge (GCD) curves of the pure SWNT cathode.

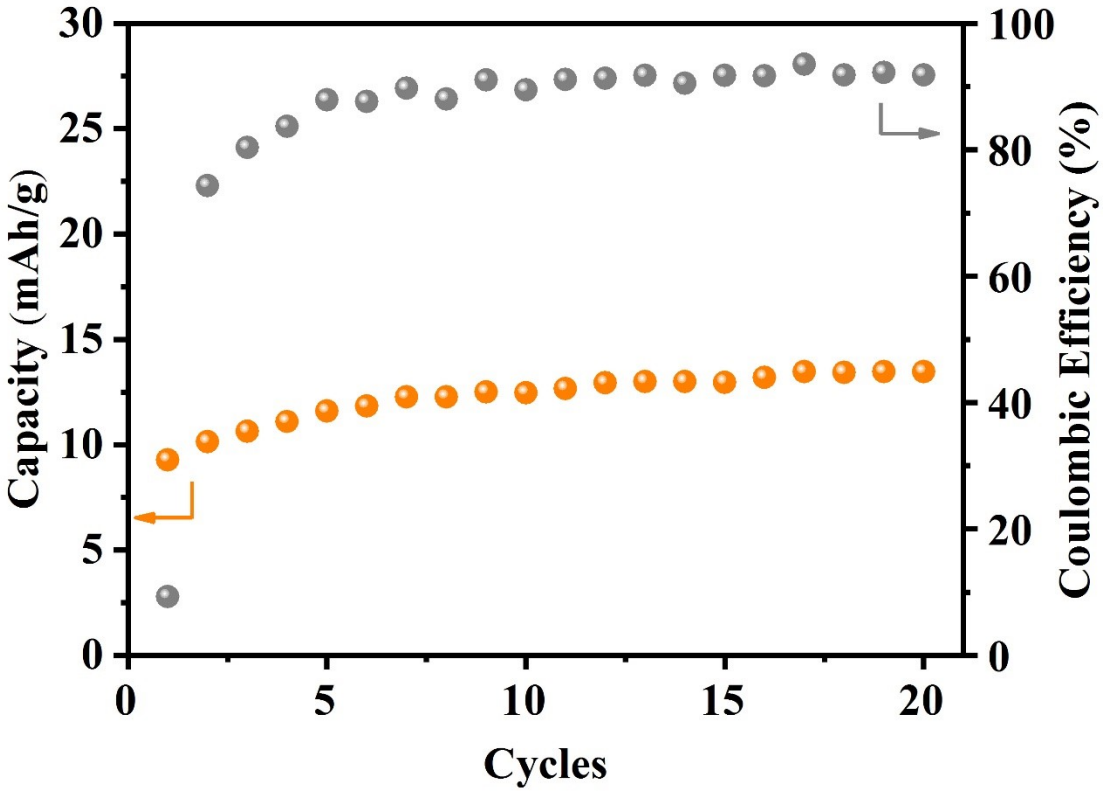

Fig. S16 Cycle performance of the pure SWNT cathode at the current density of 333 mA/g.

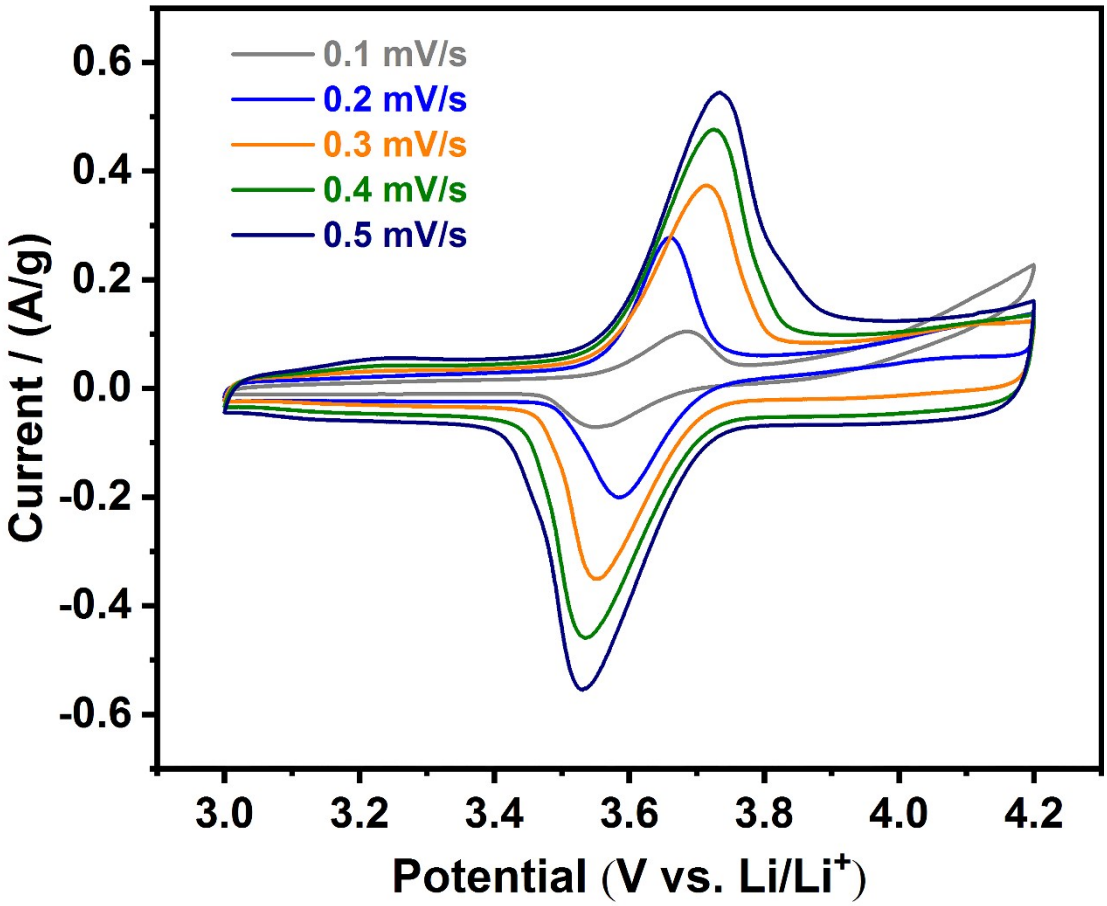

Fig. S17 CV curves of PTMA/SWNT at variant scan rates of 0.1, 0.2, 0.3, 0.4, and 0.5 mV/s.

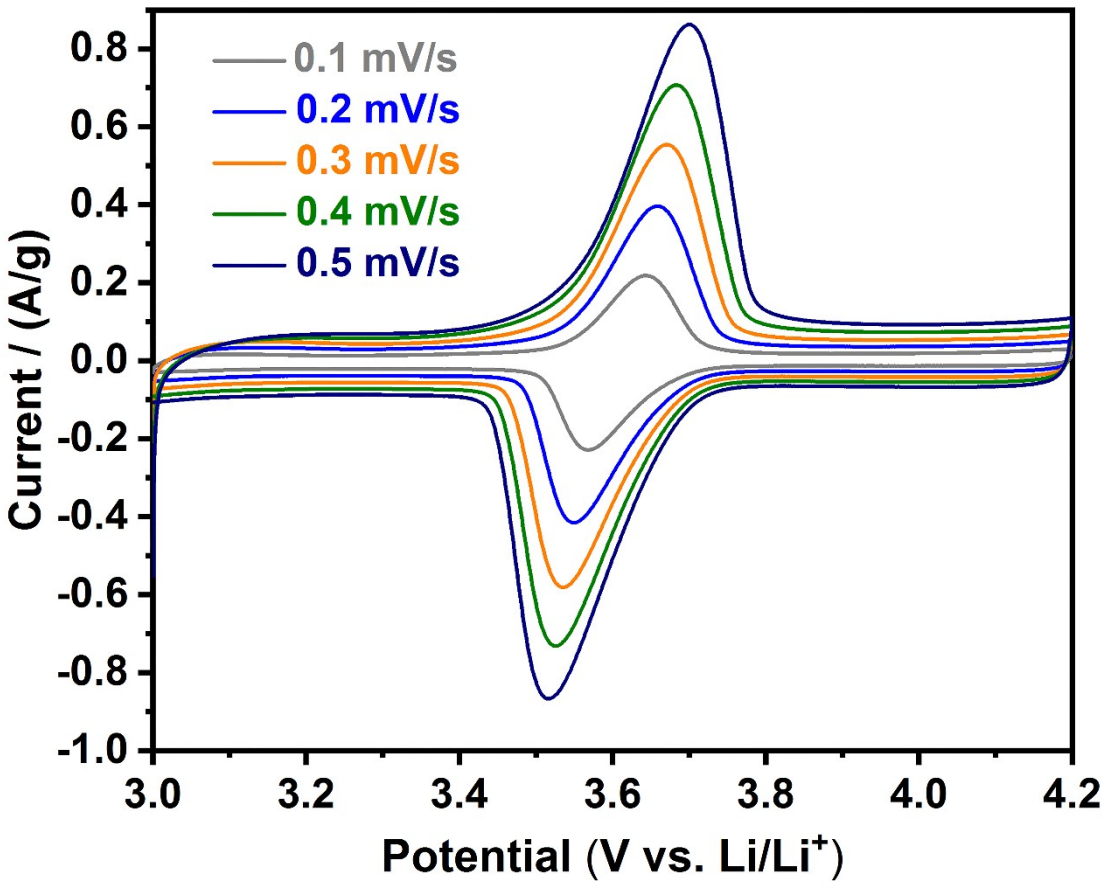

Fig. S18 CV curves of PETM/SWNT electrodes at variant scan rates of 0.1, 0.2, 0.3, 0.4, and 0.5 mV/s.

Reference

1. Y. Chen, Y. Zhang, X. Liu, X. Fan, B. Bai, K. Yang, Z. Liang, Z. Zhang and K. Mai, *Macromol. Rapid Commun.*, 2018, **39**, e1800195.
2. T. Katsumata, J. Qu, M. Shiotsuki, M. Satoh, J. Wada, J. Igarashi, K. Mizoguchi and T. Masuda, *Macromolecules*, 2008, **41**, 1175-1183.
3. W. Guo, Y.-X. Yin, S. Xin, Y.-G. Guo and L.-J. Wan, *Energy Environ. Sci.*, 2012, **5**, 5221-5225.
4. J. F. B. Gordon A. Bain, *J. Chem. Educ.*, 2008, **85**, 532-536.
5. K. Zhang, Y. Hu, L. Wang, J. Fan, M. J. Monteiro and Z. Jia, *Polym. Chem.*, 2017, **8**, 1815-1823.
6. A. Stukowski, *Model. Simul. Mater. Sc.*, 2010, **18**, 015012.